

Using TDHF to study quasifission dynamics

A. S. Umar*

Physics and Astronomy, Vanderbilt University, Nashville, TN 37235, USA

**E-mail: umar@compsci.cas.vanderbilt.edu*

C. Simenel

*Department of Nuclear Physics, The Australian National University,
Canberra ACT 2601, Australia*

We show that the microscopic TDHF approach provides an important tool to shed some light on the nuclear dynamics leading to the formation of superheavy elements. In particular, we discuss studying quasifission dynamics and calculating ingredients for compound nucleus formation probability calculations.

Keywords: TDHF; Superheavy nuclei; Quasifission

1. Introduction

The time-dependent Hartree-Fock (TDHF) theory has provided a possible means to study the diverse phenomena observed in low energy nuclear physics¹. As a result of theoretical approximations (single Slater determinant), TDHF describes reaction channels in a common mean-field, usually corresponding to the dominant reaction channel. For instance, it describes above-barrier fusion and average transfer dynamics². To obtain multiple reaction channels or widths of observables one must go beyond TDHF^{3–5}. In connection with superheavy element formation, the theory predicts best the cross-section for a particular process which dominates the reaction mechanism. This is certainly the case for studying capture cross-sections and quasifission.

In recent years has it become numerically feasible to perform TDHF calculations on a 3D Cartesian grid without any symmetry restrictions and with much more accurate numerical methods^{6,7}. During the past several years, a novel approach based on TDHF called the density constrained time-dependent Hartree-Fock (DC-TDHF) method was developed to compute heavy-ion potentials^{8,9} and excitation energies¹⁰ directly from TDHF time-evolution. This method was applied to calculate capture cross sections for

fusion reactions leading to superheavy element $Z = 112$ ¹¹. Furthermore, within the last few years the TDHF approach has been utilized for studying the dynamics of quasifission^{12–18}. The study of quasifission is showing a great promise to provide insight based on very favorable comparisons with experimental data.

2. Recent quasifission studies

One of the major questions that is asked by the experimental superheavy element community is why a ^{48}Ca beam is so crucial in forming such systems and whether one could produce new superheavy nuclei using projectiles different than ^{48}Ca and actinide targets. Our first work in this area focused on the quasifission studies for the $^{40,48}\text{Ca} + ^{238}\text{U}$ system^{12,13}, showing that for neutron-rich ^{48}Ca beams quasifission is substantially reduced. While, the above work is also in the time span of this proposal, below we discuss the more recent studies of the $^{48}\text{Ca} + ^{249}\text{Bk}$ and $^{50}\text{Ti} + ^{249}\text{Bk}$ systems¹⁴. The reaction $^{48}\text{Ca} + ^{249}\text{Bk}$ creates superheavy isotopes of element 117 with cross-sections of 2–3 picobarns. However, the $^{50}\text{Ti} + ^{249}\text{Bk}$ reaction so far has not produced any superheavy isotopes of element 119, with an upper cross-section limit of 50 fb¹⁹.

We have calculated the microscopic DC-TDHF nucleus-nucleus potential barriers for the $^{48}\text{Ca} + ^{249}\text{Bk}$ and $^{50}\text{Ti} + ^{249}\text{Bk}$ systems for two extreme orientations of the ^{249}Bk nucleus (tip and side). For the $^{48}\text{Ca} + ^{249}\text{Bk}$ system, the tip orientation of ^{249}Bk results in a significantly lower barrier, $E_B(\text{tip}) = 191.22$ MeV, as compared to the side orientation, $E_B(\text{side}) = 204.36$ MeV. This reaction has been studied at $E_{\text{c.m.}} = 204\text{--}218$ MeV in Dubna²⁰ and $E_{\text{c.m.}} = 211\text{--}218$ MeV with GSI-TASCA²¹. Thus, the highest experimental energy $E_{\text{c.m.}} = 218$ MeV is above both barriers but the lowest experimental energy $E_{\text{c.m.}} = 204$ MeV is slightly below the barrier for the side orientation of ^{249}Bk . Similarly, the corresponding potential barriers for the $^{50}\text{Ti} + ^{249}\text{Bk}$ system are $E_B(\text{tip}) = 211.2$ MeV and $E_B(\text{side}) = 224.6$ MeV. Experimentally, $E_{\text{c.m.}} = 233.2$ MeV was used in the GSI-TASCA experiment²¹, well above both barriers.

Figure 1(a) (left) shows the contact time as a function of center-of-mass energy for central collisions of ^{48}Ca with ^{249}Bk . For the tip orientation of the ^{249}Bk nucleus (dashed line) we observe contact times of order 10–12 zs which are essentially constant over a wide range of energies, $E_{\text{c.m.}} = 191\text{--}230$ MeV. Only at energies below the potential barrier, $E_B(\text{tip}) = 192.2$ MeV, do the contact times drop off very rapidly

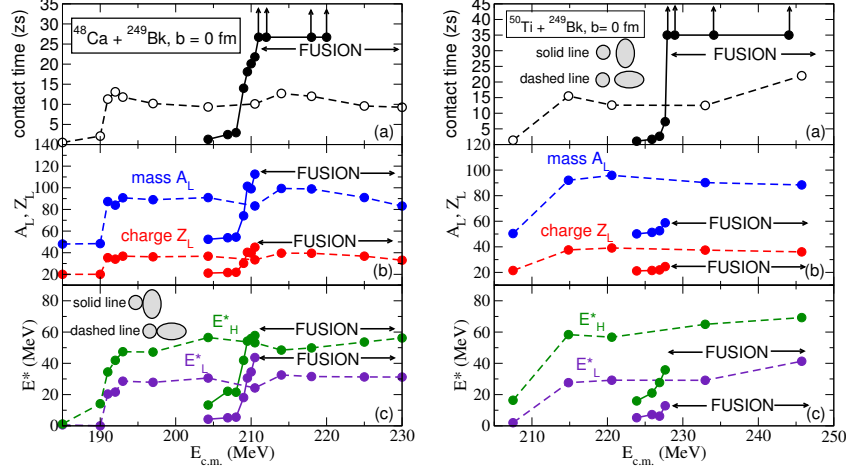


Fig. 1. (a) Contact time, (b) mass and charge of the light fragment, and (c) excitation energy E^* of the heavy and light fragments as a function of $E_{c.m.}$ for central collisions of ^{48}Ca with ^{249}Bk (left) and ^{50}Ti with ^{249}Bk (right). Solid lines are for the side orientation of the deformed ^{249}Bk nucleus, and dashed lines are for the tip orientations.

because these events correspond to inelastic scattering and few-nucleon transfer reactions. A dramatically different picture emerges for the side orientation of the ^{249}Bk nucleus (solid line): At energies above the barrier $E_B(\text{side}) = 205.4$ MeV, the contact times rise very steeply with energy and reach values up to 22 zs at $E_{c.m.} = 210$ MeV. For energies above this value, fusion is observed which we define by a large contact time exceeding 35 zs and a mononuclear shape without a neck.

Figure 1(b) (left) shows the corresponding mass and charge of the light fragment. We observe that the mass and charge transfer to the light fragment are roughly proportional to the nuclear contact time. In particular, for the side orientation of ^{249}Bk , we find quasielastic collisions at energies below $E_{c.m.} = 204$ MeV. Quasifission is limited to a small range of energies $E_{c.m.} = 209\text{--}211$ MeV, whereas for energies above 211 MeV we find fusion. Naturally, non-central impact parameters can show quasifission in the range where we see fusion. The quasifission results are very different for the tip orientation of ^{249}Bk , ranging over a much wider energy domain $E_{c.m.} = 191\text{--}230$ MeV with a lower maximum mass and charge transfer compared to the side orientation of ^{249}Bk .

We have also used DCTDHF to calculate the excitation energy of *each fragment* directly from the TDHF density evolution. This gives us new

information on the repartition of the excitation energy between the heavy and light fragments which is not available in standard TDHF calculations. In Fig. 1 (c) we show the excitation energies of the heavy and light fragments which contain approximately 55–60 MeV and 30–45 MeV of excitation energy (side orientation) and 50 MeV and 30 MeV (tip orientation), respectively, for c.m. energies corresponding to quasifission.

Right panel of Fig. 1 shows the corresponding results for central collisions of ^{50}Ti with ^{249}Bk . The contact times and the masses and charges of the light fragment show a similar behavior as a function of energy as compared to the $^{48}\text{Ca} + ^{249}\text{Bk}$ reaction. For the tip orientation, we find quasifission for $E_{\text{c.m.}} \geq 214$ MeV, with excitation energies of $E_H^* = 57\text{--}69$ MeV for the heavy fragment and $E_L^* = 27\text{--}41$ MeV for the light fragment, respectively. The mass and charge of the fragments indicate a strong influence of the shell effects in the ^{208}Pb region, as in reactions with ^{48}Ca . However, $N = 50$ does not seem to play a role here. For the side orientation, we find inelastic and multi-nucleon transfer reactions at energies $E_{\text{c.m.}} = 223\text{--}227$ MeV. Quasifission is confined to an extremely narrow energy window around $E_{\text{c.m.}} = 227.4\text{--}227.7$ MeV, with excitation energies of $E_H^* \simeq 36$ MeV and $E_L^* \simeq 13$ MeV. At energies $E_{\text{c.m.}} > 228$ MeV, fusion sets in.

3. Shape evolution and collective dynamics of quasifission

The proper characterization of fusion-fission and quasifission is one of the most important tasks in analyzing reactions leading to superheavy elements. Experimental analysis of fusion-fission and quasifission fragment angular distributions $W(\theta)$ is commonly expressed in terms of a two-component expression²²,

$$W(\theta) = \sum_{J=0}^{J_{\text{CN}}} \mathcal{F}_J^{(FF)}(\theta, K_0(FF)) + \sum_{J=J_{\text{CN}}}^{J_{\text{max}}} \mathcal{F}_J^{(QF)}(\theta, K_0(QF)). \quad (1)$$

Here, J_{CN} defines the boundary between fusion-fission and quasifission, assuming a sharp cutoff between the angular momentum distributions of each mechanism. The quantum number K is known to play an important role in fission. It is the projection of the total angular momentum onto the deformation axis. In the Transition State Model (TSM), the characteristics of the fission fragments are determined by the K distribution at scission. The argument K_0 entering Eq. (1) is the width of this distribution which is assumed to be Gaussian. It obeys $K_0^2 = T\mathfrak{S}_{eff}/\hbar^2$, where the effective moment of inertia, \mathfrak{S}_{eff} , is computed from the moments of inertia

for rotations around the axis parallel and perpendicular to the principal deformation axis $\frac{1}{\mathfrak{S}_{eff}} = \frac{1}{\mathfrak{S}_{\parallel}} - \frac{1}{\mathfrak{S}_{\perp}}$, and T is the nuclear temperature at the saddle point. The physical parameters of the fusion-fission part are relatively well known from the liquid-drop model²³. In contrast, the quasifission process never reaches statistical equilibrium. In principle, it has to be treated dynamically, while Eq. (1) is based on a statistical approximation. In addition, the usual choice for the nuclear moment of inertia for the quasifission component, $\mathfrak{S}_0/\mathfrak{S}_{eff} = 1.5$ ²⁴, is somewhat arbitrary. Here, \mathfrak{S}_0 is the moment of inertia of an equivalent spherical nucleus.

We have developed methods to extract the moment of inertia of the system (the main collective observable of interest for fission and quasifission) directly from TDHF time-evolution of collisions resulting in quasifission. The proper way to calculate the moment-of-inertia for such time-dependent densities (particularly for non-zero impact parameters) is to directly diagonalize the moment-of-inertia tensor represented by a 3×3 matrix with elements

$$\mathfrak{S}_{ij}(t)/m = \int d^3r \rho(\mathbf{r}, t)(r^2 \delta_{ij} - x_i x_j), \quad (2)$$

where ρ is the local number-density calculated from TDHF evolution, m is the nucleon mass, and $x_{i=1,2,3}$ denote the Cartesian coordinates. Numerical diagonalization the matrix \mathfrak{S} gives three eigenvalues. One eigenvalue corresponds to the moment-of-inertia \mathfrak{S}_{\parallel} for the nuclear system rotating about the principal axis. The other two eigenvalues define the moments of inertia for rotations about axes perpendicular to the principal axis. Using the time-dependent moment-of-inertia obtained from the TDHF collision one can calculate the so-called effective moment-of-inertia defined above. We have calculated the moment-of-inertia ratio for the $^{48}\text{Ca} + ^{249}\text{Bk}$ non-central collisions at $E_{c.m.} = 218$ MeV. At the point of final touching configuration the moment-of-inertia ratios are in the range 1.4-1.8, suggesting a relatively strong impact parameter dependence which should be accounted for in future extensions to the TSM.

Acknowledgments

This work has been supported by the U.S. Department of Energy under grant No. DE-SC0013847 with Vanderbilt University and by the Australian Research Councils Future Fellowship (project number FT120100760) and Discovery Projects (project number DP160101254) funding schemes.

References

1. C. Simenel, *Eur. Phys. J. A* **48**, p. 152 (2012).
2. C. Simenel and B. Avez, *Int. J. Mod. Phys. E* **17**, 31 (2008).
3. M. Tohyama and A. S. Umar, *Phys. Lett. B* **516**, 415 (2001).
4. D. Lacroix and S. Ayik, *Eur. Phys. J. A* **50**, p. 95 (2014).
5. C. Simenel, *Phys. Rev. Lett.* **106**, p. 112502 (2011).
6. A. S. Umar, M. R. Strayer, J. S. Wu, D. J. Dean and M. C. Güçlü, *Phys. Rev. C* **44**, 2512 (1991).
7. J. A. Maruhn, P.-G. Reinhard, P. D. Stevenson and A. S. Umar, *Comp. Phys. Comm.* **185**, 2195 (2014).
8. A. S. Umar and V. E. Oberacker, *Phys. Rev. C* **74**, p. 061601 (2006).
9. A. S. Umar, C. Simenel and V. E. Oberacker, *Phys. Rev. C* **89**, p. 034611 (2014).
10. A. S. Umar, V. E. Oberacker, J. A. Maruhn and P.-G. Reinhard, *Phys. Rev. C* **80**, p. 041601 (2009).
11. A. S. Umar, V. E. Oberacker, J. A. Maruhn and P.-G. Reinhard, *Phys. Rev. C* **81**, p. 064607 (2010).
12. A. Wakhle *et al.*, *Phys. Rev. Lett.* **113**, p. 182502 (2014).
13. V. E. Oberacker, A. S. Umar and C. Simenel, *Phys. Rev. C* **90**, p. 054605 (2014).
14. A. S. Umar, V. E. Oberacker and C. Simenel, *Phys. Rev. C* **94**, p. 024605 (2016).
15. A. S. Umar, V. E. Oberacker and C. Simenel, *Phys. Rev. C* **92**, p. 024621 (2015).
16. A. S. Umar and V. E. Oberacker, *Nucl. Phys. A* **944**, 238 (2015).
17. K. Hammerton *et al.*, *Phys. Rev. C* **91**, p. 041602(R) (2015).
18. K. Sekizawa and K. Yabana, *Phys. Rev. C* **93**, p. 054616 (2016).
19. C. E. Düllmann and the TASCA collaboration, in *Fission and Properties of Neutron-Rich Nuclei*, (World Scientific, 2013).
20. Y. T. Oganessian *et al.*, *Phys. Rev. C* **87**, p. 054621 (2013).
21. J. Khuyagbaatar *et al.*, *Phys. Rev. Lett.* **112**, p. 172501 (2014).
22. B. B. Back, *Phys. Rev. C* **31**, 2104 (1985).
23. A. J. Sierk, *Phys. Rev. C* **33**, 2039 (1986).
24. R. Yanez *et al.*, *Phys. Rev. C* **88**, p. 014606 (2013).